

27

Nonlinear Bifurcation Analysis

TABLE OF CONTENTS

	Page
§27.1. Introduction	27-3
§27.2. Levels of Bifurcation Analysis	27-3
§27.3. Recapitulation of Governing Equations	27-3
§27.3.1. Residual and Rate Equations	27-3
§27.3.2. Stiffness and Load Rates	27-5
§27.3.3. Limitations of λ -Parametrized Forms	27-5
§27.4. A Deeper Look at Bifurcation	27-5
§27.4.1. State Decomposition	27-5
§27.4.2. Failure of first-order rate equations at bifurcation	27-6
§27.5. Branch Analysis of Simple Bifurcation	27-6
§27.5.1. State Decomposition	27-6
§27.5.2. Finding σ	27-8
§27.6. The Hinged Cantilever	27-10
§27.6.1. Finding the Critical Point	27-11
§27.6.2. Branching Analysis	27-11
§27. Exercises.	27-14

§27.1. Introduction

We initiated our study of stability of conservative systems in Chapters 24-25 by using the simplified model of linearized prebuckling (LPB). This was followed in Chapter 26 by a qualitative study of the more general stability model that led to classifying *isolated* critical points into four types: limit point, asymmetric bifurcation, stable-symmetric bifurcation, and unstable-symmetric bifurcation. This classification is especially helpful in understanding the effect of imperfections on stability.

This Chapter presents a more detailed mathematical analysis of the phenomenon of bifurcation by studying *equilibrium branches* in the vicinity of an isolated bifurcation point. The topic is covered under the name *nonlinear bifurcation* to emphasize that we are dealing with the general case as opposed to the LPB model. A simple example involving a one-degree of freedom system is then worked out in some detail. The next Chapter takes up the subject of how physical or numerical imperfections affect structural behavior as regards both limit and bifurcation points.

§27.2. Levels of Bifurcation Analysis

Nonlinear bifurcation analysis can be carried out at different levels of detail, as demanded by the need of the application. Four levels of increasing detail are schematized in Figure 27.1, which assume the occurrence of an isolated bifurcation point B .

1. Locate: find where B occurs while tracing a response. Can be done by monitoring changes of sign of the determinant of \mathbf{K} or equivalently tracing the sign of factorization pivots (See Chapter 21).
2. Determine subspace: having located B , determine vectors \mathbf{y} (particular solution) and \mathbf{z} (null eigenvector that together with λ form an intrinsic subspace “where the action is.” Requires a partial eigensolution.
3. Branching analysis: having located B , and computed \mathbf{y} and \mathbf{z} , find the directions $\dot{\mathbf{u}}_1$ and $\dot{\mathbf{u}}_2$ of tangents to the equilibrium paths (branches) passing through B . Requires an analysis of the second order rate equations $\ddot{\mathbf{r}} = \mathbf{0}$.
4. Branch curvature analysis: having located B and determined \mathbf{y} , \mathbf{z} , $\dot{\mathbf{u}}_1$ and $\dot{\mathbf{u}}_2$, find the curvatures of the equilibrium paths (branches) passing through B . Requires an analysis of the third order equation $\ddot{\mathbf{r}} = \mathbf{0}$.

The information necessary for levels 3 is quite difficult to obtain in general purpose finite element programs, while that needed for level 4 is truly inaccessible. For this reason most FE programs can provide only levels 1 and 2 on a routine basis. In the present Chapter we study up to level 3 (branching analysis), but the practical difficulties of implementing that level should be kept in mind.

§27.3. Recapitulation of Governing Equations

Below we recapitulate discrete governing equations derived in Chapters 3 and 4, and introduce additional nomenclature required for the branching analysis carried out in §27.4.

§27.3.1. Residual and Rate Equations

The one-parameter residual equilibrium equations are

$$\mathbf{r}(\mathbf{u}, \lambda) = \mathbf{0}, \quad (27.1)$$

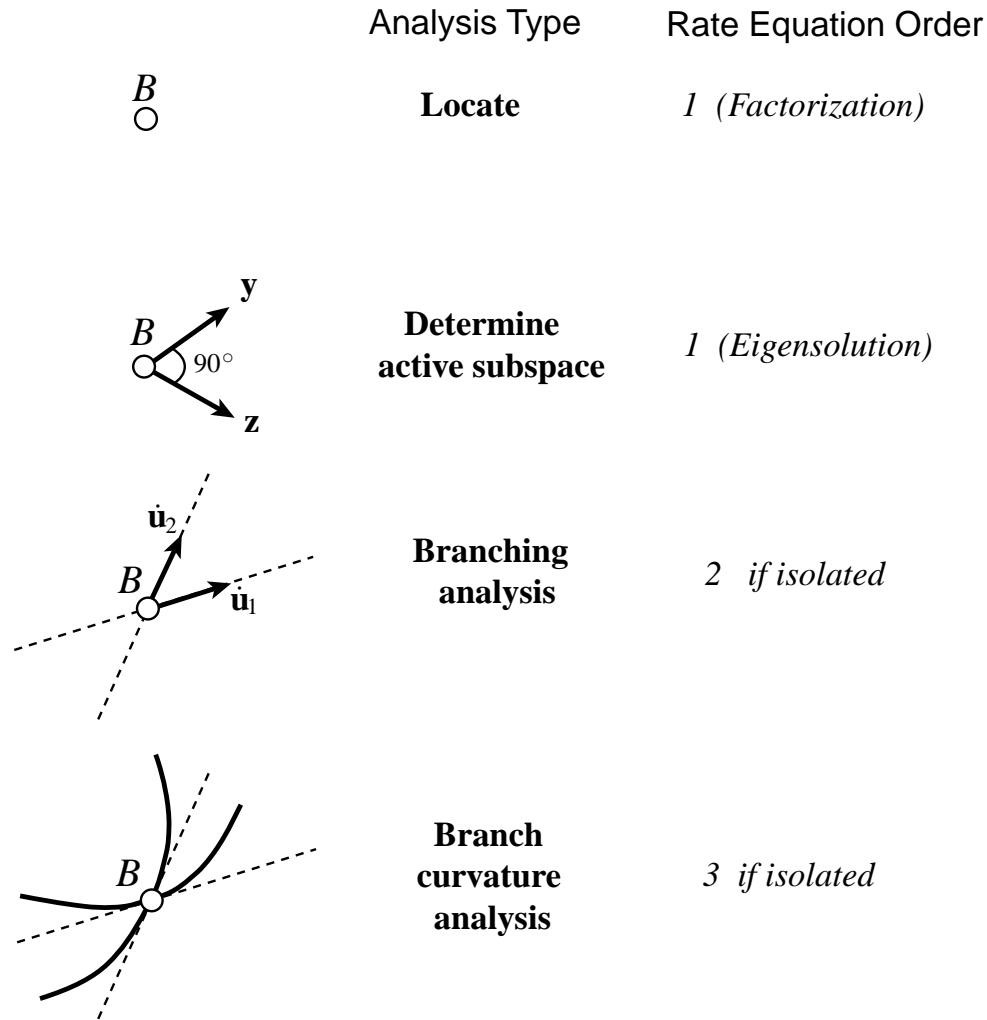


Figure 27.1. The four levels of information for nonlinear bifurcation analysis.

where λ is the stage control parameter and \mathbf{u} is the state vector. Solutions of this equation may be conveniently represented in parametric form

$$\mathbf{u} = \mathbf{u}(t), \quad \lambda = \lambda(t), \quad (27.2)$$

where t is a dimensionless path parameter. Two important special choices for pseudotime are

$$t = \lambda, \quad t = s, \quad (27.3)$$

which leads to the λ -*parametrized* and *arclength* forms, respectively.

Rate equations are systems of ordinary differential equations obtained by successive differentiation of (27.1) with respect to t . Recall that \mathbf{K} and \mathbf{q} denote the tangent stiffness matrix and incremental load vector, respectively, whose entries are given by

$$K_{ij} = \frac{\partial r_i}{\partial u_j}, \quad q_i = \frac{\partial r_i}{\partial \lambda}. \quad (27.4)$$

Using superposed dots to denote t -differentiation we obtain

$$\dot{\mathbf{r}} = \mathbf{K}\dot{\mathbf{u}} - \mathbf{q}\dot{\lambda} = \mathbf{0}, \quad (27.5)$$

$$\ddot{\mathbf{r}} = \mathbf{K}\ddot{\mathbf{u}} + \dot{\mathbf{K}}\dot{\mathbf{u}} - \dot{\mathbf{q}}\dot{\lambda} - \mathbf{q}\ddot{\lambda} = \mathbf{0}, \quad (27.6)$$

$$\dddot{\mathbf{r}} = \mathbf{K}\ddot{\mathbf{u}} + \dot{\mathbf{K}}\ddot{\mathbf{u}} + \ddot{\mathbf{K}}\dot{\mathbf{u}} - \mathbf{q}\ddot{\lambda} - \dot{\mathbf{q}}\ddot{\lambda} - \ddot{\mathbf{q}}\dot{\lambda} = \mathbf{0}. \quad (27.7)$$

and so on. Eq. (27.5) is a system of first-order rate equations, also called the *incremental stiffness equations* or simply the *stiffness equations*. Eq. (27.6) is a system of second-order rate equations, also called the *stiffness-rate equations*. Eq. (27.7) is a system of third-order rate equations, and so on. For the branching analysis undertaken here we will go up to the second-rate equations (27.6).

§27.3.2. Stiffness and Load Rates

In the second-order system (27.6), the stiffness matrix rate $\dot{\mathbf{K}}$ and incremental load vector rate $\dot{\mathbf{q}}$ may be expressed as linear combinations of $\dot{\mathbf{u}}$ and $\dot{\lambda}$:

$$\dot{\mathbf{K}} = \mathbf{L}\dot{\mathbf{u}} + \mathbf{N}\dot{\lambda}, \quad \dot{\mathbf{q}} = -(\mathbf{N}\dot{\mathbf{u}} + \mathbf{a}\dot{\lambda}) \quad (27.8)$$

The entries of these new matrices and vectors are given by

$$L_{ijk} = \frac{\partial^2 r_i}{\partial u_j \partial u_k}, \quad N_{ij} = \frac{\partial^2 r_i}{\partial u_j \partial \lambda} = \frac{\partial K_{ij}}{\partial \lambda}, \quad a_i = \frac{\partial^2 r_i}{\partial \lambda \partial \lambda} = \frac{\partial q_i}{\partial \lambda}. \quad (27.9)$$

Remark 27.1. Note that \mathbf{L} is a three-dimensional array which may be called a *cubic matrix* to distinguish it from an ordinary square matrix. Postmultiplying a cubic matrix by a vector yields an ordinary matrix. For example $\mathbf{L}\dot{\mathbf{u}}$ is a matrix.

§27.3.3. Limitations of λ -Parametrized Forms

If one chooses $t = \lambda$, simplifications take place in systems (27.5)-(27.7) because $\dot{\lambda} = 1$ and $\ddot{\lambda} = \ddot{\lambda} = 0$. Using primes to denote differentiation with respect to λ , the first two rate forms reduce to

$$\mathbf{K}\mathbf{u}' - \mathbf{q} = \mathbf{0}, \quad (27.10)$$

$$\mathbf{K}\mathbf{u}'' + \mathbf{K}'\mathbf{u}' - \mathbf{q}' = \mathbf{0}, \quad (27.11)$$

in which

$$\mathbf{K}' = \mathbf{L}\mathbf{u}' + \mathbf{N}, \quad \mathbf{q}' = -(\mathbf{N}\mathbf{u}' + \mathbf{a}). \quad (27.12)$$

These forms are unsuitable, however, near a bifurcation point, because there the relationship between \mathbf{u} and λ ceases to be unique, and the more general parametrized forms such as (27.6) must be used.

§27.4. A Deeper Look at Bifurcation

At critical points \mathbf{K} becomes singular and therefore possesses at least one null eigenvector, which as usual is called \mathbf{z} . This eigenvector will be *normalized to unit length*. As discussed in Chapter 5, if the eigenvector is orthogonal (non-orthogonal) to the incremental load vector, the critical point is a bifurcation (limit) point.

§27.4.1. State Decomposition

The conditions for bifurcation may be summarily stated as

$$\mathbf{K}\mathbf{z} = \mathbf{0}, \quad \|\mathbf{z}\| = \mathbf{z}^T \mathbf{z} = 1, \quad \mathbf{q}^T \mathbf{z} = 0. \quad (27.13)$$

Because the structural system is assumed to be conservative, \mathbf{K} is symmetric. Consequently \mathbf{z} is also a left eigenvector of $\mathbf{K} = \mathbf{K}^T$. In structural mechanics, the eigenvector \mathbf{z} is called a *buckling mode* or *buckling shape*. This term conveys the idea that the structure jumps from a prebuckling state into the new shape. Although the name is appropriate in the LPB model, we shall see that it is not necessarily appropriate in the general case.

At the bifurcation point B the state vector \mathbf{u} and the control parameter λ assume values \mathbf{u}_B and λ_B , respectively. As in Chapter 25 we study *small* deviations of \mathbf{u} and λ in the neighborhood of B . These deviations are denoted by $\Delta\mathbf{u} = \mathbf{u} - \mathbf{u}_B$ and $\Delta\lambda = \lambda - \lambda_B$, respectively. For small deviations from the bifurcation point the relation between $\Delta\mathbf{u}$ and $\Delta\lambda$ may be linearized as

$$\Delta\mathbf{u} = (\sigma\mathbf{z} + \mathbf{y})\Delta\lambda, \quad (27.14)$$

where \mathbf{y} is the *particular solution* introduced in §25.2, and σ is the *buckling mode amplitude*.

Dividing by $\Delta\lambda$ and passing to the limit $\Delta\lambda \rightarrow 0$ we obtain the rate form of the above equation:

$$\dot{\mathbf{u}} = (\sigma\mathbf{z} + \mathbf{y})\dot{\lambda}. \quad (27.15)$$

This decomposition of $\dot{\mathbf{u}}$ in the \mathbf{y}, \mathbf{z} plane is depicted in Figure 27.2, a duplicate of Figure 25.1.

§27.4.2. Failure of first-order rate equations at bifurcation

At bifurcation points the first-order rate equations (27.5) *yield no information on the buckling mode amplitude*. This is worked out in Exercise 25.3, which shows that $\sigma = 0/0$ and is therefore indeterminate. To get deterministic information in the vicinity of a bifurcation point it is necessary to use information from *higher-order rate equations*. This is covered in the following subsection for a isolated (simple, distinct) bifurcation point. For this case the second-order rate equations (27.6) are usually sufficient.

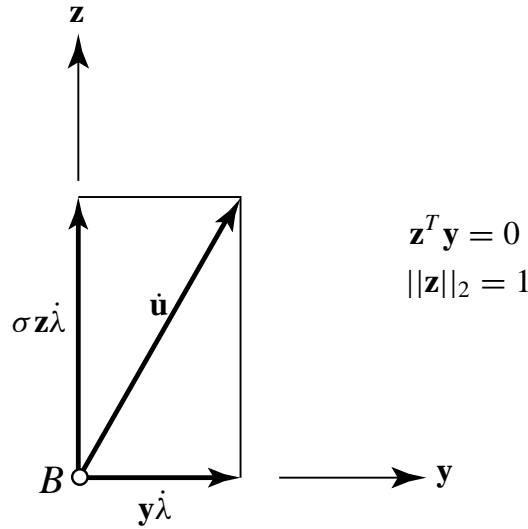


Figure 27.2. State decomposition at isolated bifurcation point B , depicted in the (y, z) plane.

§27.5. Branch Analysis of Simple Bifurcation

The subsequent analysis assumes that the rank deficiency of \mathbf{K} at bifurcation is only one, and so \mathbf{z} is the only null eigenvector. This is called an *isolated, simple* or *distinct* bifurcation point. We shall see that at such points there can be at most *two* equilibrium paths that intersect at B . Such paths are called *branches*.

§27.5.1. State Decomposition

Assume that we have located a bifurcation point B and computed the buckling mode \mathbf{z} . Our next task is to examine the structural behavior in the *neighborhood* of B . This analysis is important to answer questions pertaining to the *safety* of the structure and its sensitivity to imperfections.

We have seen that the state variation rate $\dot{\mathbf{u}}$ from the bifurcation point can be decomposed into a *homogeneous solution* component $\sigma\mathbf{z}$ in the buckling mode direction, and a *particular solution* component \mathbf{y} , which is orthogonal to \mathbf{z} :

$$\dot{\mathbf{u}} = (\mathbf{y} + \sigma\mathbf{z})\dot{\lambda}, \quad \mathbf{y}^T\mathbf{z} = 0 \quad (27.16)$$

See the geometric interpretation in Figure 27.2.

The particular solution vector \mathbf{y} solves the system

$$\mathbf{K}\mathbf{y} = \mathbf{q}, \quad \mathbf{z}^T\mathbf{y} = 0, \quad (27.17)$$

which is simply the first-order incremental flow equation augmented by a normality constraint. Imposing this constraint removes the singularity (rank deficiency) of \mathbf{K} at B .

Remark 27.2. The homogeneous solution \mathbf{z} lies in the null space of \mathbf{K} whereas the particular solution \mathbf{y} lies in the range space of \mathbf{K} . In more physical terms we may say that \mathbf{y} “responds” to the load (the incremental load vector \mathbf{q}) whereas \mathbf{z} , like any homogeneous solution, is dictated by the boundary conditions.

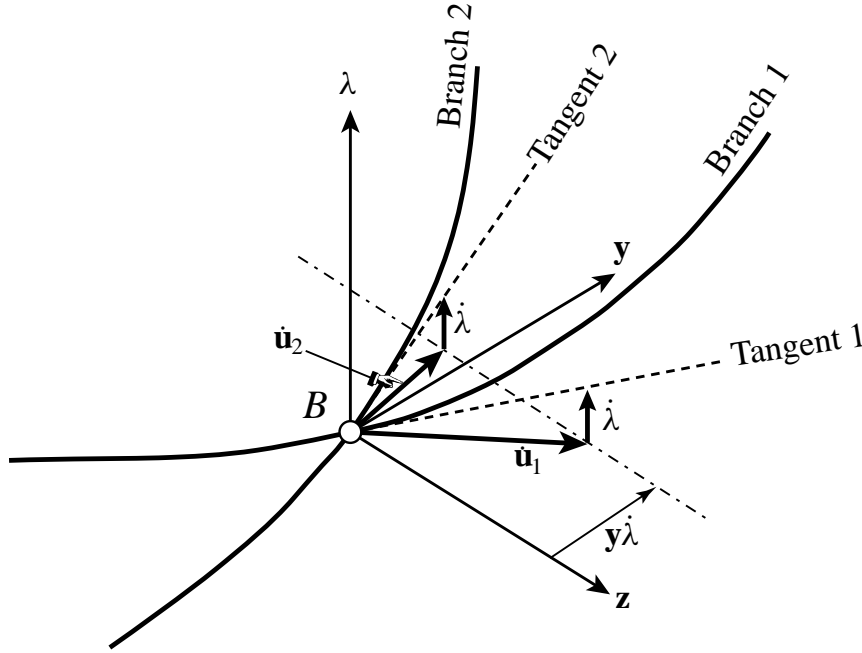


Figure 27.3. Intersection of two equilibrium paths at an isolated bifurcation point B , depicted in the (y, z, λ) subspace.

Remark 27.3. The decomposition (27.16) is analogous in many respects to the decomposition of element motions into purely-deformational and rigid-body, studied in Chapter 10. Here z take the role of rigid body mode. The decomposition (27.16) is, however, expressed in terms of rates because it is *local*: it is restricted to the vicinity of the bifurcation point.

§27.5.2. Finding σ

The first-level information on the equilibrium branches at B is given by their *tangents* at B . Because we can obtain y and z from the first-order rate equations, these tangents are fully determined if in addition we know σ , \dot{u} and $\dot{\lambda}$ at B .

But as noted previously the first-order rate equations (27.5) do not provide information on the buckling mode amplitude σ . To get that information it is necessary to go to the second-order system (27.6), which is repeated here for convenience:

$$\mathbf{K}\ddot{u} + \dot{\mathbf{K}}\dot{u} - \mathbf{q}\ddot{\lambda} - \dot{\mathbf{q}}\dot{\lambda} = 0 \quad (27.18)$$

Premultiplying both sides by \mathbf{z}^T and taking account of the bifurcation conditions (27.13) we get at B the scalar equation

$$\mathbf{z}^T \dot{\mathbf{K}}\dot{u} - \mathbf{z}^T \dot{\mathbf{q}}\dot{\lambda} = 0 \quad (27.19)$$

Replacement of $\dot{\mathbf{K}}$ and $\dot{\mathbf{q}}$ by the expressions (27.8) gives

$$\mathbf{z}^T (\mathbf{L}\dot{u} + \mathbf{N}\dot{\lambda})\dot{u} + \mathbf{z}^T (\mathbf{N}\dot{u} + \mathbf{a}\dot{\lambda})\dot{\lambda} = 0. \quad (27.20)$$

Finally, substitution of \dot{u} by its homogeneous-plus-particular decomposition (27.16) yields

$$\mathbf{z}^T [\mathbf{L}(\mathbf{y} + \sigma\mathbf{z})\dot{\lambda} + \mathbf{N}\dot{\lambda}] (\mathbf{y} + \sigma\mathbf{z})\dot{\lambda} + \mathbf{z}^T [\mathbf{N}(\mathbf{y} + \sigma\mathbf{z})\dot{\lambda} + \mathbf{a}\dot{\lambda}] \dot{\lambda} = 0. \quad (27.21)$$

Removing the common differential factor $(\dot{\lambda})^2$ and collecting terms in σ we arrive at the quadratic equation

$$a\sigma^2 + 2b\sigma + c = 0, \quad (27.22)$$

in which

$$a = \mathbf{z}^T \mathbf{L} \mathbf{z} \mathbf{z}, \quad b = \mathbf{z}^T [\mathbf{L} \mathbf{z} \mathbf{y} + \mathbf{L} \mathbf{y} \mathbf{z} + 2\mathbf{N} \mathbf{z}], \quad c = \mathbf{z}^T [\mathbf{L} \mathbf{y} \mathbf{y} + 2\mathbf{N} \mathbf{y} + \mathbf{a}]. \quad (27.23)$$

This quadratic equation generally provides two roots: σ_1 and σ_2 . In what follows we shall assume that these two roots are real (see Remark 27.5 below).

Substitution of σ_1 and σ_2 into (27.16) furnishes the *branching directions* at the bifurcation point:

$$\dot{\mathbf{u}}_1 = (\mathbf{y} + \sigma_1 \mathbf{z}) \dot{\lambda}, \quad \dot{\mathbf{u}}_2 = (\mathbf{y} + \sigma_2 \mathbf{z}) \dot{\lambda}. \quad (27.24)$$

These are sketched in Figure 27.3 in the three-dimensional space $(\mathbf{y}, \mathbf{z}, \lambda)$ with origin at B . Figure 27.4 projects this picture onto the (\mathbf{y}, \mathbf{z}) plane for additional clarity.

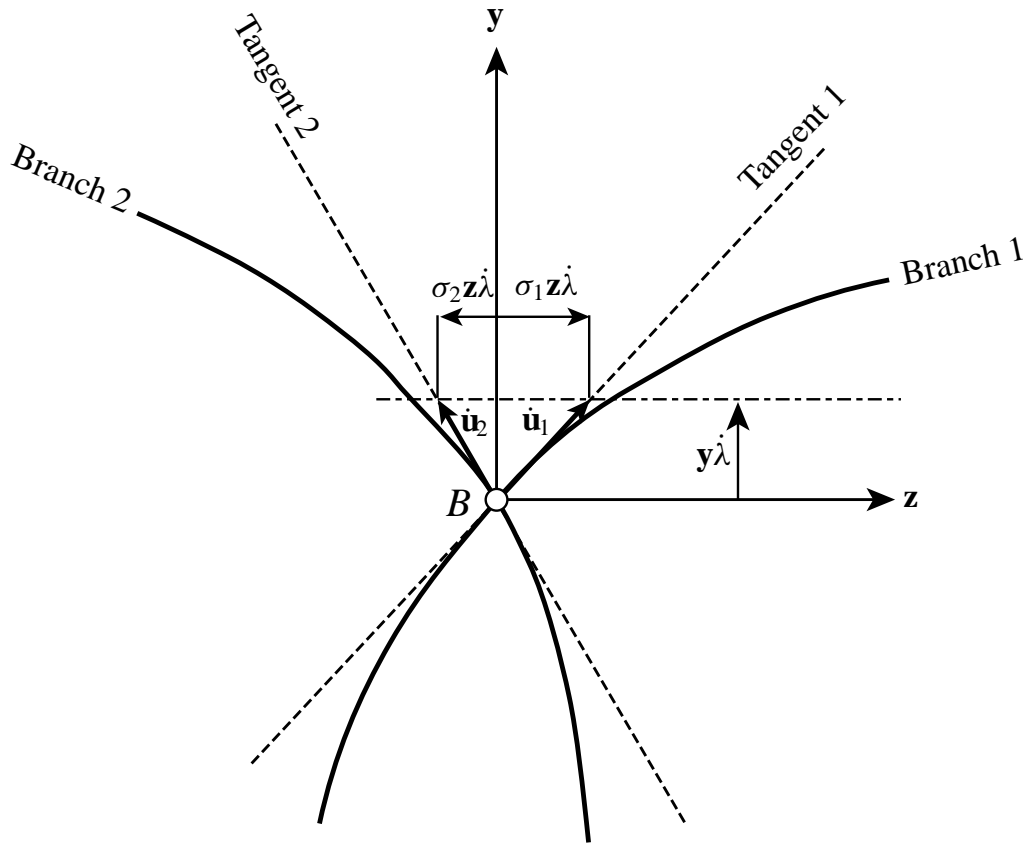


Figure 27.4. Same as Figure 27.3 but looking down the λ axis onto the (\mathbf{y}, \mathbf{z}) plane.

The key result of this subsection is that *there are at most two branches emanating from a simple bifurcation point*. The classification of such points into asymmetric and symmetric bifurcation points according to the values of σ_1 and σ_2 appears in the Exercises. In the following section an illustrative example is worked out by hand.

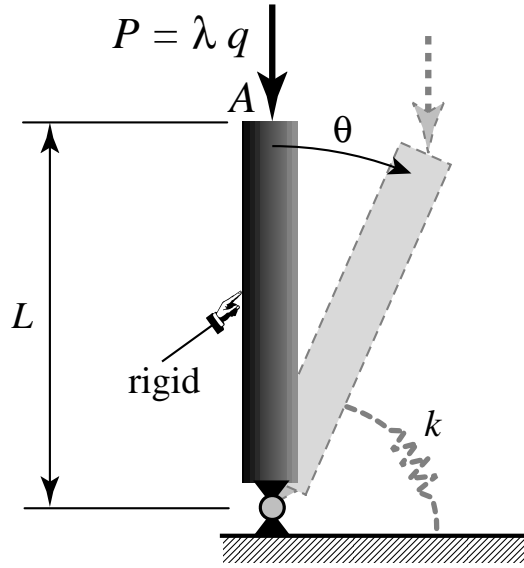


Figure 27.5. The hinged cantilever.

Remark 27.4. If $a = 0$ one root, say σ_2 , becomes infinite while the other is $\sigma_1 = -c/(2b)$, assuming $b \neq 0$. Then $\dot{\mathbf{u}}_2$ becomes aligned with \mathbf{z} . Only in this case it is justified to call \mathbf{z} the “buckling mode.”

Remark 27.5. Intuitively it appears that the two roots of (27.22) must be real. The argument goes as follows: one of the two branches is supposed to exist since B has been located by hypothesis on the equilibrium path. Its tangent at B must therefore correspond to one of the roots of (27.22). Since one of the roots is by hypothesis real, the other must also be real because a , b and c are real coefficients.

This indirect proof is not intellectually satisfying, especially to a mathematician. It would be preferable to prove the root reality by direct reasoning. However the writer has not been able to find such a proof in the literature, and personal efforts (one hour trying) have been so far unrewarding.

Remark 27.6. If $a = b = c = 0$ the second-order rate form (27.6) does not provide any local information as regards branches at B . Then one must continue to the third order rate form (27.7). This will give a cubic equation in σ with four real coefficients. Since such an equation can have one or three real roots, things get far more complicated. If all four coefficients vanish, one must go to the fourth-order rate form, and so on. (For a mathematician specialized in this kind of analysis, hell is a place where the first one million rate forms yield no information.)

§27.6. The Hinged Cantilever

The branch analysis technique is illustrated on the hinged-cantilever problem depicted in Figure 27.5. A rigid rod of length L supported by a torsional spring of stiffness k is axially loaded by a dead force $P = \lambda q$, $q = k/L$. Note that k has the physical dimension of force \times length, *i.e.* of a moment. Hence the definition $P = \lambda k/L$ renders λ dimensionless, which is convenient for hand analysis.

The dimensionless stage control parameter is $\lambda = PL/k$. As state parameter we chose the tilt angle θ as most appropriate for hand analysis. The total potential energy is

$$\Pi = U - V = \frac{1}{2}k\theta^2 - Pu = \frac{1}{2}k\theta^2 - PL(1 - \cos \theta) = k \left[\frac{1}{2}\theta^2 - \lambda(1 - \cos \theta) \right]. \quad (27.25)$$

The equilibrium equation in terms of θ is

$$r = \frac{\partial \Pi}{\partial \theta} = k(\theta - \lambda \sin \theta) = 0, \quad (27.26)$$

This has the two solutions

$$\theta = 0, \quad \lambda = \frac{\theta}{\sin \theta}, \quad (27.27)$$

which pertain to the primary (vertical or untilted) and secondary (tilted) equilibrium paths, respectively. The two paths intersect at $\lambda = 1$, which is therefore a bifurcation point.

§27.6.1. Finding the Critical Point

The incremental equation in terms of θ is

$$K\dot{\theta} - q\dot{\lambda} = 0, \quad (27.28)$$

with

$$K = \frac{\partial r}{\partial \theta} = k(1 - \lambda \cos \theta), \quad q = -\frac{\partial r}{\partial \lambda} = k \sin \theta. \quad (27.29)$$

On the primary path, $\theta = 0$, the stiffness vanishes at

$$\lambda = 1, \quad \text{or} \quad P = k/L. \quad (27.30)$$

On this path the stiffness is positive (negative) if $\lambda < 1$ ($\lambda > 1$), respectively. On the secondary path, $\lambda = \theta / \sin \theta$, the stiffness is given by

$$K = k \left(1 - \frac{\theta \cos \theta}{\sin \theta} \right), \quad (27.31)$$

which vanishes at $\theta = 0$ because $\theta / \sin \theta \rightarrow 1$ as $\theta \rightarrow 0$. If $\theta \neq 0$, $K > 0$. The various cases as regards the sign of K are summarized in Figure 27.6. Because K is a scalar, positive and negative values corresponds to stable and unstable equilibrium, respectively, with neutral stability at B . Stable (unstable) paths are shown with full (dashed) lines.

It is seen that $\theta = 0^\circ$ and $\lambda = 1$ is the only point at which K vanishes, and consequently is the only critical point. Let us verify now that the critical point is a bifurcation point. Since the system has only one degree of freedom, the normalized null eigenvector is simply the scalar $z = 1$, and the inner product $\mathbf{z}^T \mathbf{q}$ reduces to

$$zq = q = k \sin \theta \quad (27.32)$$

which vanishes at $\theta = 0^\circ$. Consequently ($\lambda = 1, \theta = 0^\circ$) is a bifurcation point.

§27.6.2. Branching Analysis

In this problem the particular solution \mathbf{y} vanishes because there is only one degree of freedom. We may therefore take

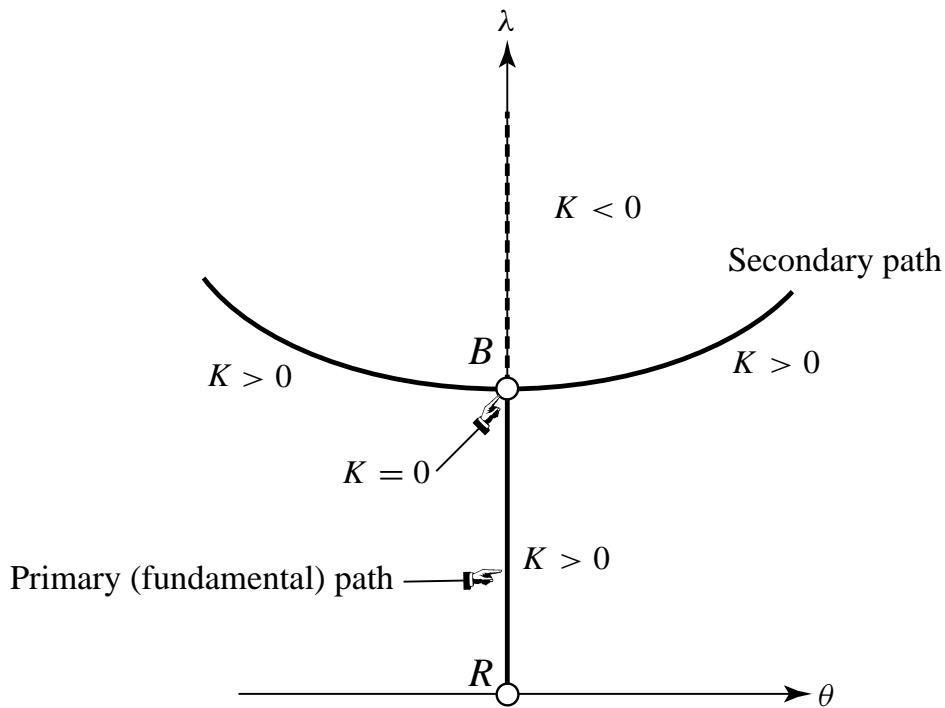
$$\dot{\theta} = \sigma \mathbf{z} \dot{\lambda} = \sigma \dot{\lambda} \quad (27.33)$$

The second-order rate equation is

$$\lambda \sin \theta \dot{\theta} \dot{\theta} - 2 \cos \theta \dot{\theta} \dot{\lambda} = 0,$$

which upon substituting $\dot{\theta} = \sigma \dot{\lambda}$ yields the quadratic equation (27.22) with $a = \lambda \sin \theta$, $b = -2$, $c = 0$. At the bifurcation point ($\lambda = 1, \theta = 0$) we get

$$0 \cdot \sigma^2 - 2\sigma = -2\sigma = 0 \quad (27.34)$$

Figure 27.6. The sign of the stiffness coefficient K for the hinged cantilever response.

The two roots of (27.34) as a quadratic equation are

$$\sigma_1 = 0, \quad \sigma_2 = \infty, \quad (27.35)$$

leading to the solutions

$$\dot{\theta} = 0, \quad \dot{\lambda} = 0. \quad (27.36)$$

These branches are the tangents to the primary (vertical bar) and secondary (tilted bar), respectively, at the bifurcation point. See Figure 27.7.

This Figure also sketches the post-buckling response, which for this problem is easily obtained from the exact equilibrium solutions (27.27). According to the qualitative classification of Chapter 26, the bifurcation point is of stable-symmetric type. This subclassification of a symmetric bifurcation point into stable and unstable cannot be discerned, however, from the branch-tangent analysis, because it requires information on the *curvature* of the \mathbf{z} -directed branch.

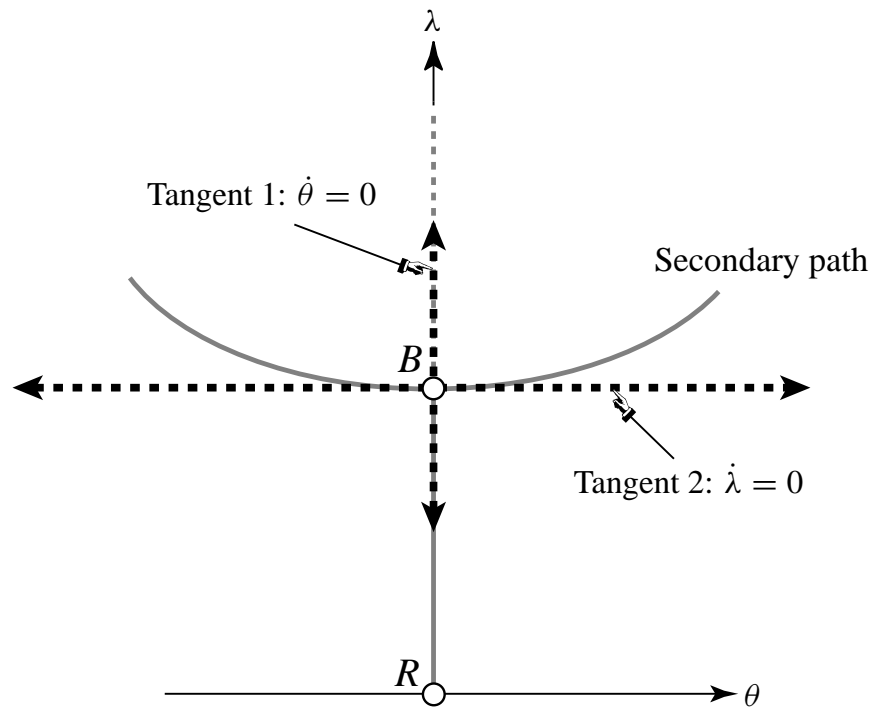


Figure 27.7. The two branch directions at bifurcation point of the hinged cantilever.

Homework Assignments for Chapter 27

Nonlinear Bifurcation Analysis

EXERCISE 27.1 [A:15] Consider

$$\mathbf{L} = \frac{\partial \mathbf{K}}{\partial \mathbf{u}}, \quad \mathbf{N} = \frac{\partial \mathbf{K}}{\partial \lambda}, \quad \mathbf{a} = -\frac{\partial \mathbf{q}}{\partial \lambda}. \quad (\text{E27.1})$$

Are these relations true?

EXERCISE 27.2 [A:20] If $a \rightarrow 0$ in the quadratic equation (27.22) while $b \neq 0$, one of the roots, say σ_1 , goes to ∞ whereas the other one becomes $\sigma_2 = -c/2b$. This is called a *symmetric* bifurcation. Show that in such a case the branch direction corresponding to σ_1 coincides with the buckling mode \mathbf{z} , and draw a bifurcation diagram similar to Figure 27.1.

EXERCISE 27.3 [A:40] Algebraically prove that the roots of the quadratic equation (27.5) are real¹

EXERCISE 27.4 [A:25] The LPB first order rate equations are $\dot{\mathbf{r}} = \mathbf{K}\dot{\mathbf{u}} - \mathbf{q}\dot{\lambda} = \mathbf{0}$, in which $\mathbf{K} = \mathbf{K}_0 + \lambda\mathbf{K}_1$ and where \mathbf{K}_0 , \mathbf{K}_1 and \mathbf{q} are constant. Using Exercise 25.3 (posted solution), show that LPB can only predict symmetric bifurcation. What wonderful thing happens if $\mathbf{K}_1\mathbf{y} = \mathbf{0}$?

EXERCISE 27.5 [A:20] The *propped cantilever* shown in Figure 28.3 consists of a *rigid* bar of length L pinned at A and supported by a linear extensional spring of stiffness k . The spring is assumed to be capable of resisting both tension and compression and retains its horizontal orientation as the system deflects. The bar may rotate all the way around the pin. The rigid bar is subjected to a vertical dead load P that remains vertical. Define dimensionless control and state parameters as

$$\lambda = \frac{P}{kL}, \quad \mu = \sin \theta. \quad (\text{E27.2})$$

Analyze the stability of the propped cantilever in a manner similar to §27.5. Show that the secondary equilibrium path is the circle $\lambda^2 + \mu^2 = 1$ and sketch the response paths showing the complete circle. From this diagram, can you tell whether the bifurcation point at $\lambda = 1$ is stable-symmetric or unstable-symmetric? How about the one at $\lambda = -1$?

¹ A very difficult assignment worth of a paper. I am not aware of anybody that has done for the general case.